Biochimica et Biophysica Acta 1824 (2012) 1024–1030

Contents lists available at SciVerse ScienceDirect

Biochimica et Biophysica Acta

journal homepage: www.elsevier.com/locate/bbapap

The structural basis for the narrow substrate specificity of an acetyl esterase from *Thermotoga maritima*

Matthew K. Hedge [a], Alexandra M. Gehring [a], Chinessa T. Adkins [b], Leigh A. Weston [a], Luke D. Lavis [b], R. Jeremy Johnson [a,*]

[a] Department of Chemistry, Butler University, 4600 Sunset Ave, Indianapolis, IN 46208, USA
[b] Janelia Farm Research Campus, The Howard Hughes Medical Institute, 19700 Helix Dr, Ashburn, VA 20147, USA

ARTICLE INFO

Article history:
Received 11 April 2012
Received in revised form 9 May 2012
Accepted 22 May 2012
Available online 1 June 2012

Keywords:
Acetyl esterase
Cephalosporin-C deacetylase
Fluorogenic enzyme substrates
Hydrolases
Substrate specificity

ABSTRACT

Acetyl esterases from carbohydrate esterase family 7 exhibit unusual substrate specificity. These proteins catalyze the cleavage of disparate acetate esters with high efficiency, but are unreactive to larger acyl groups. The structural basis for this distinct selectivity profile is unknown. Here, we investigate a thermostable acetyl esterase (TM0077) from *Thermotoga maritima* using evolutionary relationships, structural information, fluorescent kinetic measurements, and site directed mutagenesis. We measured the kinetic and structural determinants for this specificity using a diverse series of small molecule enzyme substrates, including novel fluorogenic esters. These experiments identified two hydrophobic plasticity residues (Pro228, and Ile276) surrounding the nucleophilic serine that impart this specificity of TM0077 for small, straight-chain esters. Substitution of these residues with alanine imparts broader specificity to TM0077 for the hydrolysis of longer and bulkier esters. Our results suggest the specificity of acetyl esterases have been finely tuned by evolution to catalyze the removal of acetate groups from diverse substrates, but can be modified by focused amino acid substitutions to yield enzymes capable of cleaving larger ester functionalities.

1. Introduction

The α/β hydrolases together with the oxidoreductases and transferases represent 75% of the known enzymes encoded by all genomes [1]. Biochemists and chemists have long appreciated the expansive reaction and substrate scope contained within the α/β hydrolase superfamily [2–4]. This broad specificity originates from the same α/β hydrolase protein fold and utilizes the same catalytic triad, suggesting great plasticity and generality in this privileged structure [3,5]. This broad specificity, however, complicates the prediction of endogenous substrates and biological functions of α/β hydrolases [1,2,5].

Among α/β hydrolases, the acetyl esterase subclass from carbohydrate esterase family 7 (CE7) (EC 3.1.1.6) exhibits a distinct combination of narrow substrate specificity for acetate esters, but broad substrate specificity for disparate alcohol moieties [6–8]. The broad substrate specificity for alcohols is highlighted by the range of acetylated substrates that are hydrolyzed by CE7 acetyl esterases, including cephalosporins, glucose pentaacetate, *p*-nitrophenyl acetate, 4-methylumbelliferyl acetate, and α/β-naphthyl acetate (Fig. 1A) and by their position independence to hydrolysis of β-D-xylopyranoside monoacetates [8–11]. The three-dimensional structures of CE7 acetyl esterases from *Bacillus pumilus* (PDB ID: 2XLB), *Bacillus subtilis* (PDB ID: 1ODS), and *Thermotoga maritima* (PDB ID: 1VLQ; 3M81; 3M82; 3M83) show the presence of a cavernous substrate-binding pocket lined with large hydrophobic amino acids [6,8,12]. This large substrate-binding pocket contains sufficient space to accommodate diverse substrates and provides an explanation for the broad substrate specificity of acetyl esterases to a range of alcohols [6,8,12]. Current structural or enzymatic data do not, however, account for the distinctively narrow substrate specificity of CE7 acetyl esterases for acetate esters and the inability of acetyl esterases to catalyze reactions besides deacetylations.

In this study, we measure the precise reactivity of TM0077, a cytoplasmic CE7 acetyl esterase from *T. maritima*, toward libraries of disparate alcohol- and ester-containing substrates. We synthesize a series of chemically stable diacyloxymethyl ether fluorescein derivatives to measure the precise substrate specificity of TM0077 for diverse esters. Utilizing the kinetics of these reactions, the three-dimensional structures of TM0077, and the evolutionary conservation of binding pocket residues, we identify the structural and enzymatic features of acetyl esterases that maintain their unique combination of broad substrate specificity for alcohols, but narrow substrate specificity for acetate esters.

Abbreviations: 7-ACA, 7-aminocephalosporanic acid; BTB, bromothymol blue; CE7, carbohydrate esterase family 7; DSF, differential scanning fluorimetry; LB, Luria–Bertani broth; MWCO, molecular weight cut-off; Ni-NTA, nickel-nitrilotriacetic acid; NPA, 4-nitrophenol acetate; PDB, protein data bank; TM0077, acetyl esterase from *Thermotoga maritima*

* Corresponding author at: Butler University, 4600 Sunset Ave., Indianapolis, IN, 46208, USA. Tel.: +1 317 940 9062; fax: +1 317 940 9519.
E-mail address: rjjohns1@butler.edu (R.J. Johnson).

1570-9639/$ – see front matter © 2012 Elsevier B.V. All rights reserved.
doi:10.1016/j.bbapap.2012.05.009

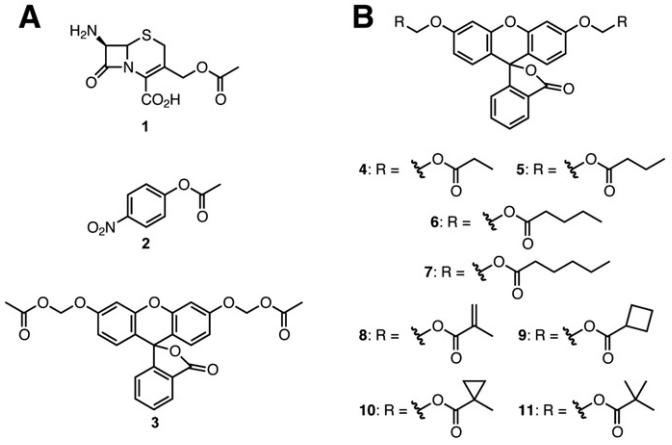

Fig. 1. Compounds used to measure substrate specificity: A) Broad specificity. Three model substrates (**1**: 7-amino cephalosporanic acid, **2**: *p*-nitrophenyl acetate, and **3**: fluorescein di(acetoxymethyl ether) were used to determine the substrate specificity of TM0077 for different alcohol substituents. B) Narrow specificity. Fluorogenic esterase substrates (substrates **3**–**11**) were used to characterize the specificity of TM0077 for esters, including its ability to accept varying acyl chains (substrates **3**–**7**) and increased steric bulk and steric hindrance (substrates **8**–**11**). All substrates have fluorescein and an acyloxymethyl ether with varying R groups.

2. Materials and methods

2.1. General synthesis

Fluorogenic enzyme substrates **3**, **4**, and **8**–**11** were synthesized as previously described [13]. All reagents were the highest grade available and obtained from Sigma–Aldrich or Fisher Scientific. Preactivated, powdered 4-Å molecular sieves from Sigma–Aldrich were used as received. Anhydrous solvents were drawn from Aldrich Sure-Seal bottles. Thin-layer chromatography was performed by using aluminum-backed plates coated with silica gel containing F_{254} phosphor and visualized by UV-illumination, charring, or staining with I_2, ceric ammonium molybdate, or phosphomolybdic acid. Column chromatography was performed on an Isolera 4 system with SNAP columns (Biotage). The term "concentrated *in vacuo*" refers to the removal of solvents and other volatile materials by using a rotary evaporator with a controlled diaphragm pump (≥1 mm Hg) while maintaining the water-bath temperature below 40 °C. NMR spectra were obtained with a Bruker 400 MHz Avance-II$^+$ spectrometer at the Janelia Farm Research Campus. ^{1}H and ^{13}C NMR spectra were referenced to tetramethylsilane or residual solvent peaks. ^{13}C NMR spectra hydrogen multiplicity (C, CH, CH_2, CH_3) information was obtained from DEPT spectra.

2.2. Fluorescein dibutyloxymethyl ether (5)

The following procedure for **5** is representative. To a solution of tetrabutylammonium hydrogensulfate (274 mg, 0.808 mmol, 0.1 equiv) and potassium carbonate (4.47 g, 32.3 mmol, 4.0 equiv) in 10 mL H_2O and 10 mL CH_2Cl_2 was added butyric acid (740 μL, 8.08 mmol, 1.0 equiv) and a solution of chloromethyl chlorosulfate (1.23 mL, 12.12 mmol, 1.5 equiv) in 5 mL CH_2Cl_2. The reaction was stirred vigorously (~600 RPM) at room temperature under N_2(g) for 4 h. The mixture was then diluted to 30 mL H_2O and 50 mL CH_2Cl_2 and the layers were separated. The aqueous layer was extracted with 2 × 50 mL CH_2Cl_2, the organic layers were combined and dried over $MgSO_4$, filtered, and concentrated *in vacuo*. Note: material is extremely volatile. The residue was filtered through a plug of silica gel, washed with 100 mL CH_2Cl_2, and concentrated *in vacuo*, affording chloromethyl butyrate as a colorless liquid (637 mg, 58%). ^{1}H NMR (400 MHz, $CDCl_3$) δ 5.71 (s, 2H), 2.37 (t, J = 7.4 Hz, 2H), 1.77–1.62 (m, 2H), 0.97 (t, J = 7.4 Hz, 3H). ^{13}C NMR (101 MHz, $CDCl_3$) δ 171.59 (C), 68.53 (CH_2), 35.81 (CH_2), 18.06 (CH_2), 13.46 (CH_3).

Chloromethyl butyrate (540 mg, 3.95 mmol, 4.0 eq) was dissolved in HPLC-grade acetone (4.0 mL). NaI (592 mg, 3.95 mmol, 4.0 eq) was added and the reaction mixture was stirred for 24 h at ambient temperature under N_2(g). The white precipitate was removed via filtration (celite) and the resulting yellow solution was concentrated *in vacuo*. The dark yellow viscous oil was purified via column chromatography (silica gel, 4 → 34% v/v EtOAc in hexanes containing constant 20% v/v CH_2Cl_2 as cosolvent) to yield a pale yellow oil. This material was taken up in anhydrous CH_3CN (6.0 mL) under N_2(g). Fluorescein (328 mg, 0.988 mmol, 1.0 eq), powdered 4-Å molecular sieves (300 mg), and anhydrous Ag_2O (572 mg, 2.46 mmol, 2.5 eq) were added, and the reaction mixture was stirred for 48 h at ambient temperature. The reaction mixture was then diluted with CH_2Cl_2 (100 mL) and filtered (celite). The resulting solution was concentrated *in vacuo* to give a yellow-brown oil and purified via column chromatography (silica gel, 3 → 28% v/v EtOAc in hexanes containing constant 20% v/v CH_2Cl_2 as cosolvent) affording **3** as a white solid (186 mg, 35%). ^{1}H NMR (400 MHz, $CDCl_3$) δ 8.03 (d, J = 7.5 Hz, 1H), 7.68 (dd, J = 7.2, 7.0 Hz, 1H), 7.63 (dd, J = 7.3, 7.3 Hz, 1H), 7.16 (d, J = 7.6 Hz, 1H), 7.01–6.90 (m, 2H), 6.80–6.65 (m, 4H), 5.79 (s, 4H), 2.36 (t, J = 7.4 Hz, 4H), 1.77–1.60 (m, 4H), 0.95 (t, J = 7.4 Hz, 6H). ^{13}C NMR (101 MHz, $CDCl_3$) δ 172.41 (C), 169.22 (C), 158.44 (C), 152.97 (C), 152.24 (C), 135.10 (CH), 129.88 (CH), 129.36 (CH), 126.67 (C), 125.17 (CH), 123.88 (CH), 113.28 (C), 112.74 (CH), 103.55 (CH), 84.83 (CH_2), 82.46 (C), 36.01 (CH_2), 18.17 (CH_2), 13.55 (CH_3).

2.3. Fluorescein divaleryloxymethyl ether (6)

Data for chloromethyl valerate: (70%, colorless oil). ^{1}H NMR (400 MHz, $CDCl_3$) δ 5.70 (s, 2H), 2.39 (t, J = 7.5 Hz, 2H), 1.73–1.58 (m, 2H), 1.46–1.28 (m, 2H), 0.93 (t, J = 7.3 Hz, 3H). ^{13}C NMR (101 MHz, $CDCl_3$) δ 171.51 (C), 68.30 (CH_2), 33.44 (CH_2), 26.32 (CH_2), 21.81 (CH_2), 13.36 (CH_3). Data for **4**: (44%, white solid). ^{1}H NMR (400 MHz, $CDCl_3$) δ 8.07–7.99 (m, 1H), 7.68 (ddd, J = 7.5, 7.4, 1.4 Hz, 1H), 7.63 (ddd, J = 7.4, 7.3, 1.2 Hz, 1H), 7.19–7.11 (m, 1H), 7.01–6.90 (m, 2H), 6.80–6.65 (m, 4H), 5.79 (s, 4H), 2.38 (t, J = 7.5 Hz, 4H), 1.70–1.57 (m, 4H), 1.41–1.29 (m, 4H), 0.89 (t, J = 7.3 Hz, 6H). ^{13}C NMR (101 MHz, $CDCl_3$) δ 172.58 (C), 169.21 (C), 158.43 (C), 152.98 (C), 152.24 (C), 135.09 (CH), 129.87 (CH), 129.36 (CH), 126.66 (C), 125.17 (CH), 123.87 (CH), 113.27 (C), 112.74 (CH), 103.55 (CH), 84.83 (CH_2), 82.44 (C), 33.87 (CH_2), 26.69 (CH_2), 22.14 (CH_2), 13.64 (CH_3).

2.4. Fluorescein dicaproyloxymethyl ether (7)

Data for chloromethyl caproate: (76%, colorless oil). ^{1}H NMR (400 MHz, $CDCl_3$) δ 5.70 (s, 2H), 2.38 (t, J = 7.5 Hz, 2H), 1.75–1.59 (m, 2H), 1.45–1.21 (m, 4H), 1.03–0.80 (m, 3H). ^{13}C NMR (101 MHz, $CDCl_3$) δ 171.77 (C), 68.55 (CH_2), 33.94 (CH_2), 31.07 (CH_2), 24.20 (CH_2), 22.22 (CH_2), 13.82 (CH_3). Data for **5**: (13%, white solid). ^{1}H NMR (400 MHz, $CDCl_3$) δ 8.07–7.97 (m, 1H), 7.67 (ddd, J = 7.5, 7.4, 1.4 Hz, 1H), 7.63 (ddd, J = 7.4, 7.3, 1.2 Hz, 1H), 7.19–7.09 (m, 1H), 7.02–6.88 (m, 2H), 6.81–6.65 (m, 4H), 5.79 (s, 4H), 2.37 (t, J = 7.5 Hz, 4H), 1.74–1.57 (m, 4H), 1.38–1.19 (m, 8H), 0.96–0.77 (m, 6H). ^{13}C NMR (101 MHz, $CDCl_3$) δ 172.59 (C), 169.20 (C), 158.42 (C), 152.98 (C), 152.23 (C), 135.08 (CH), 129.87 (CH), 129.36 (CH), 126.66 (C), 125.17 (CH), 123.86 (CH), 113.27 (C), 112.74 (CH), 103.52 (C), 84.81 (CH_2), 82.43 (C), 34.13 (CH_2), 31.15 (CH_2), 24.35 (CH_2), 22.26 (CH_2), 13.85 (CH_3).

2.5. TM0077 purification

A bacterial expression plasmid (pMH1) containing the TM0077 gene from *T. maritima* (UniprotKB: Q9WXT2; protein name TM0077) was obtained from the Harvard Plasmid Repository (Clone ID: TmCD00083900). This bacterial plasmid was transformed into *Escherichia coli* BL21 (DE3) RIPL cells (Agilent, La Jolla, CA). A saturated overnight culture of *E. coli* BL21 (DE3) RIPL (pMH1-

TM0077) in LB media containing ampicillin (100 μg/mL) and chloramphenicol (30 μg/mL) was used to inoculate LB-media (100 mL) containing ampicillin (100 μg/mL) and chloramphenicol (30 μg/mL) and the bacterial culture was grown with constant shaking (225 rpm) at 37 °C. When the OD_{600} reached 0.6–0.8, L-arabinose (Alfa-Aesar, Ward Hill, MA) was added to 0.2% w/v and protein induction proceeded for 3 h. Bacterial cultures were collected by centrifugation at 6000 ×*g* for 10 min at 4 °C. The bacterial cell pellet was resuspended in PBS (2 mL) and stored at −20 °C.

To disrupt the bacterial cell wall, lysozyme (50 mg; Sigma-Aldrich, St. Louis, MO) was added and incubated with the cell pellet for 30 min at 25 °C. The disrupted cell pellet was transferred to a 65 °C water bath and incubated for 60 min. Precipitated proteins and cell material were removed by centrifugation at 16,000 ×*g* for 10 min at 25 °C. Ni-NTA agarose (500 μL; Qiagen, Valencia, CA) was added to the soluble fraction and allowed to incubate at 25 °C for 15 min. The resin was washed three times with PBS containing increasing concentrations of imidazole (1 mL each of PBS containing 10 mM imidazole, 25 mM imidazole, or 50 mM imidazole) and recollected by centrifugation at 1000 ×*g* for 1 min at 25 °C. TM0077 was eluted in PBS containing 250 mM imidazole (600 μL) and dialyzed against PBS overnight at 4 °C with constant stirring (10 K MWCO; Pierce, Rockford, IL).

The purity of TM0077 was confirmed by SDS–PAGE on a 4–20% gradient gel and the purity was shown to be greater than 95% (Supplementary Fig. 1). The concentration of TM0077 was determined by measuring the absorbance at 280 nm and by calculating the extinction coefficient ($\varepsilon^{280} = 55810\ M^{-1}\ s^{-1}$ with all free cysteines) using the modified Edelhoch and Gill/Von Hippel methods on Expasy [14–16].

2.6. Site-directed mutagenesis and purification

Variants of TM0077 were created by Quikchange II site-directed mutagenesis using the manufacturer's suggested procedure (Agilent, Santa Clara, CA) and the mutagenesis primers outlined in Supplementary Table 1. Proper mutations in the TM0077 DNA sequence were confirmed by DNA sequencing (Genewiz, South Plainfield, NJ). Plasmids with TM0077 variants were transformed into *E. coli* BL21 (DE3) RIPL cells and variants of TM0077 were purified using the same procedure as for wild-type TM0077 (Supplemental Fig. 1). For variants of TM0077 with tyrosine and tryptophan substitutions, the extinction coefficients were adjusted to correct for the loss of a chromophore (Tyr $\varepsilon^{280} = 54320\ M^{-1}\ s^{-1}$; Trp $\varepsilon^{280} = 50310\ M^{-1}\ s^{-1}$) [14–16].

2.7. Fluorescent enzymatic assays

The enzymatic activity of TM0077 was measured against flurogenic substrates (Fig. 1) using a 96-well microplate assay [13]. Fluorogenic substrates were prepared as stock solutions in DMSO (10 mM) were diluted into PBS containing BSA (PBS–BSA; 0.1 mg/mL) to a starting concentration of 10 μM. Eight serial dilutions (1:2; 60 μL into 180 μL total volume) of each substrate (10 μM–4.6 nM final concentrations) were made using PBS–BSA. Fluorogenic substrate dilutions (95 μL) were transferred to a black 96-well microplate (Corning, Lowell, MA).

TM0077 or variants of TM0077 (5 μL of 30 μg/mL) were added to the diluted fluorogenic substrates in the 96-well microplate (100 μL final volume and final TM0077 concentration = 1.5 μg/mL) and the fluorescence change ($\lambda_{ex} = 485$ nm, $\lambda_{em} = 528$ nm) was measured for 4 min at 25 °C on a Biotek Synergy 2 fluorescent plate reader (Biotek Instruments; Winooski, VT). The fluorescence change was converted to molar concentrations using a fluorescein standard curve (30 nM–0.23 nM), whose fluorescence was determined simultaneously. The initial rates of the reactions were measured in triplicate and plotted versus fluorogenic enzyme substrate concentration. The saturation enzyme kinetic traces were fitted to a standard Michaelis–Menten equation using Origin 6.1 (OriginLab Corp., Northhampton, MA) and values for k_{cat}, K_M and k_{cat}/K_M calculated. The background fluorescence of substrates **3**–**11** was determined by measuring the kinetics of fluorogenic substrate hydrolysis by an active site knockout of TM0077 (S188A).

2.8. Enzymatic activity against substrate **1** (7-aminocephalosporanic acid)

The enzymatic activity of TM0077 toward substrate **1** (7-amino cephalosporanic acid; 7-ACA; Sigma-Aldrich, St. Louis, MO; Fig. 1A) was determined by following a previously published method [10]. Briefly, the deacetylation of substrate **1** by TM0077 was determined by measuring the change in pH over time using the pH indicator bromothymol blue (BTB; Sigma-Aldrich, St. Louis, MO). Serial dilutions (1:2) of substrate **1** (300 mM–0.14 mM final concentrations) were made in 5 mM phosphate buffer pH 7.3 containing 0.01% BTB and the serial dilutions transferred to a 96-well clear microplate (95 μL). To start the reaction, TM0077 or variants of TM0077 (5 μL of a 2 mg/mL solution) were added to a final concentration of 0.1 mg/mL. Plates were preshaken for 30 s to insure complete mixing and the change in absorbance at 630 nm was measured for 5 min at 25 °C in a Biotek Synergy 2 fluorescent plate reader (Biotek Instruments; Winooski, VT). The initial velocity of the reaction was calculated using the following equation:

$$M/\min = (dA/dT) \times ((C_B + C_{In})/C_{In}) \times (1/(\Delta\varepsilon \times l)$$

where C_B is the molar concentration of buffer (0.005 M), C_{In} is the molar concentration of indicator (16 nM), $\Delta\varepsilon$ is the difference in the extinction coefficient between protonated and deprotonated BTB ($\Delta\varepsilon_{630} = 15{,}700\ M^{-1}\ cm^{-1}$), and l is the pathlength (1 cm). Values for k_{cat}, K_M, and k_{cat}/K_M were determined by fitting the hyperbolic curve of substrate **1** concentrations versus initial velocity to a standard Michaelis–Menten equation using Origin 6.1.

2.9. Enzymatic activity against substrate **2** (p-nitrophenol acetate)

The enzymatic activity of TM0077 was measured against substrate **2** (*p*-nitrophenol acetate; NPA; Sigma–Aldrich; St. Louis, MO; Fig. 1B) using a 96-well microplate assay [11]. Substrate **2** was prepared as stock solutions in acetonitrile (2 M) and diluted into PBS containing BSA (PBS–BSA; 0.1 mg/mL) to a starting concentration of 20 mM. Eight serial dilutions (1:1; 110 μL into 220 μL total volume; 20 mM–156 μM final concentrations) were made using PBS–BSA containing 1% acetonitrile. Substrate **2** dilutions (95 μL) were transferred to a clear 96-well microplate (Corning, Lowell, MA).

TM0077 or variants of TM0077 (5 μL of 30 μg/mL) were added to the diluted substrate **2** in the 96-well microplate (100 μL final volume and final TM0077 concentration = 1.5 μg/mL) and the absorbance change (412 nm) was measured for 4 min at 25 °C on a Biotek Synergy 2 fluorescent plate reader (Biotek Instruments; Winooski, VT). The absorbance change was converted to molar concentrations using the extinction coefficient of NPA ($\Delta\varepsilon_{412} = 1.4\ mM^{-1}\ cm^{-1}$). The initial rates of the reactions were measured in triplicate and plotted versus substrate **2** concentration. The saturation enzyme kinetic traces were fitted to a standard Michaelis–Menten equation using Origin 6.1 (OriginLab Corp., Northhampton, MA) and values for k_{cat}, K_M and k_{cat}/K_M calculated.

2.10. Thermal stability measurements

Similar to previously published methods [17,18], the thermal stability of TM0077 and variants of TM0077 was determined using differential scanning fluorimetry (DSF). Wild-type TM0077 and variants of TM0077 (0.5 mg/mL) were diluted in triplicate in PBS containing a 1:1000 dilution of Sypro Ruby (Invitrogen, Carlsbad, CA). The samples was heated from 50 °C to 100 °C at 2 °C/min in a thermocycler (Bio-rad C1000 Thermocylcer with CFX96 Real-time System, Hercules, CA) and the

change in Sypro Ruby fluorescence followed over time ((λ_{ex} = 450–490 nm, λ_{em} = 610–650 nm). The melting temperature (T_m) was determined by plotting the first derivative of fluorescence versus temperature and finding the temperature at the midpoint of the transition. As in previous analyses [17], all graphs were normalized so that minimum fluorescence was set to 0 and maximum fluorescence set to 1 (Supplemental Fig. 4).

2.11. Sequence alignment

The sequence alignment of bacterial acetyl xylan esterases was completed using the standard parameters for ClustalW 2.0.12 [19]. The sequences used in the alignment were from *T. maritima* (UniprotKB: Q9WXT2), *Thermotoga neapolitana* (UniprotKB: B9K758), *Streptomyces coelicolor* (UniprotKB: Q9FC27), *B. subtilis* (UniprotKB: P94388), *B. pumilus* (UniprotKB: Q9K5F2), *Thermoanaerobacterium* (UniprotKB: O30361), *Enterococcus faecalis* (UniprotKB: Q835Y2), *Clostridium perfringens* (UniprotKB: Q8XK07), *Streptococcus pneumoniae* (UniprotKB: Q97PE0), and *Leptospira interrogans* (UniprotKB: Q8F524).

3. Results and discussion

3.1. Determination of substrate specificity

Most bacterial esterases and lipases show broad substrate specificity, highlighted by their ability to catalyze the hydrolysis of aliphatic esters with varying structures [2,20,21]. Acetyl esterases also display broad specificity and catalyze the deacetylation of a broad range of substrates irrespective of the alcohol scaffold [8–11]. Yet, based on the binding of the irreversible suicide inhibitors paraoxon and phenylmethylsulfonyl fluoride and enzymatic activity measurements using *p*-nitrophenyl propionate and *p*-nitrophenyl butyrate, acetyl esterases were known to be highly specific for acetate substrates, not possessing the structural space available to accommodate larger ester substrates [8,12,22].

To provide a comprehensive evaluation of the specificity of the thermostable acetyl esterase TM0077, we utilized two distinct groups of substrates (Fig. 1). To confirm the broad substrate specificity of TM0077 for the alcohols substituents, ester hydrolysis by TM0077 was measured against three acetate-based substrates: 7-aminocephalosporonic acid (7-ACA, **1**), *p*-nitrophenyl acetate (NPA, **2**), and fluorescein di(acetoxymethyl ether) (**3**) (Fig. 1A). This group of substrates consists of alcoholic functionalities with diverse complexity and steric hindrance that closely mimic the size and polarity of its natural sugar substrates [8]. To probe the narrow substrate selectivity of TM0077 for esters, we synthesized a focused series of esterase substrates all based on the fluorescein scaffold (Fig. 1B). These nine fluorogenic enzyme substrates examined the ability of TM0077 to adapt to slight differences in carbon chain length (substrates **4**–**7**), to accommodate steric bulk and changes in electronic structure (substrates **8** and **9**), and to cleave esters with quaternary α-carbons (substrates **10** and **11**). Compared to common ester substrates, including *p*-nitrophenyl esters and fluorescein diacetate, the diacyloxymethyl ether fluorescein substrates have significantly improved chemical stability, which increases the sensitivity of the enzymatic measurements and permits measurement of even very low enzymatic rates (Table 1 and Fig. 2A) [13].

Kinetic measurements show TM0077 is active against all three acetyl substrates (**1**–**3**; Fig. 1A) with k_{cat}/K_M values that vary by only three-fold ($830\ M^{-1}\ s^{-1}$ for substrate **1** to $2.3\times10^4\ M^{-1}\ s^{-1}$ for substrate **2**; Table 1), confirming its broad specificity irrespective of the alcohol scaffold. Experiments using a series of diverse ester substrates (compounds **3**–**11**; Fig. 1B) show that TM0077 displays a strong preference for acetate groups. Nevertheless, the high chemical stability of the fluorescein substrates enabled determination of k_{cat}/K_M values for each substrate (Table 1; Fig. 2A). Increasing the carbon chain by a single carbon (substrate **4**) from the acetate ester (substrate **3**) decreases the catalytic rate by 2.2-fold; the catalytic activity continues to drop substantially with each additional carbon (substrates **5**–**7**). Fig. 2B clearly illustrates the very narrow substrate specificity of TM0077 even for similar straight chain esters. Although the K_M values shift slightly with carbon chain length, the majority of the decreased catalytic efficiency is caused by a substantial decrease in substrate turnover (k_{cat}) (Fig. 2C). As the steric hindrance surrounding the ester carbonyl increases from substrate **8** to substrate **11**, the enzymatic efficiency also decreases significantly, again caused by decreased substrate turnover with the hydrolysis of substrate **11** falling below the detection limit of the experiment (Table 1). Substitution of Ser188 with alanine completely abolished the activity of TM0077 against substrate **3** and defined a background level of substrate hydrolysis for each substrate (Supplemental Fig. 2). These results confirm the proposed specificity of TM0077, as it is able to catalyze the rapid hydrolysis of a range of substrates independently of the alcohol moiety, but with narrow selectivity for acetate esters.

Table 1
Kinetic values for ester hydrolysis of substrates **1**–**11** by TM0077.

Substrate	K_m (μM)	k_{cat}/K_m ($M^{-1}\ s^{-1}$)
1[a]	20800 ± 350	830 ± 150
2[b]	760 ± 100	23000 ± 3200
3[c]	3.7 ± 0.2	14100 ± 800
4	0.97 ± 0.2	6400 ± 1400
5	0.41 ± 0.1	15 ± 4
6	1.0 ± 0.2	1.5 ± 0.3
7	2.6 ± 0.7	0.40 ± 0.11
8	0.51 ± 0.04	140 ± 10
9	0.96 ± 0.2	23 ± 5
10	0.54 ± 0.07	4.6 ± 1.4
11[d]	N/A	N/A

[a] Kinetic constants for substrate **1** (7-ACA) were determined by measuring the change in pH due to acetate release during substrate **1** hydrolysis. Kinetic measurements for each substrate were repeated three times and the values are given ± SE. Data were fitted to a standard Michaelis–Menten equation to determine the values for k_{cat}, K_M, and k_{cat}/K_M.
[b] Kinetic constants for substrate **2** (NPA) were determined by measuring the change in A_{412} due to acetate release.
[c] Kinetic constants for substrates **3**–**11** were determined by measuring the increase in fluorogenic substrate fluorescence over time [13].
[d] Kinetic constant values for the cleavage of substrate **11** by TM0077 were below the detection limit.

The substrate turnover (k_{cat}) value measured for the hydrolysis of substrate **3** by TM0077 is slower than the turnover of substrates **1** and **2** and likely reflects the pK_a value of the hemiacetal leaving group on substrate **3**, estimated to be similar to formaldehyde hydrate (pK_a = 12.78) [13]. Thus, hydrolysis of the acyl-enzyme intermediate formed between TM0077 and substrate **3** would be much slower than the hydrolysis of the intermediate formed with *p*-nitrophenol acetate (pK_a = 7.18) [6,13]. This stability in the ester bond is necessary to maintain the extremely low background hydrolysis of these fluorogenic substrates [13,23]. The lower K_M value for substrate **3** may also signify that the hydrolysis of the acyl-enzyme intermediate is the rate-determining step in the reaction, instead of the formation of the covalent acyl-enzyme intermediate [6]. Although the relative values for k_{cat} and K_M for TM0077 hydrolysis of substrate **3** shifts from substrates **1** and **2**, the overall ratio of enzymatic catalysis k_{cat}/K_M remains fairly constant for acetate esters (Table 1).

3.2. Structural basis for substrate specificity

To determine the substrate binding residues that contribute to the unusual substrate specificity of TM0077, the positioning and sequence conservation of potential substrate-binding residues were characterized. Crystal structures of TM0077 from *T. maritima* (PDB ID: 1VLQ; 3M81; 3M82; 3M83) depict a deep and well-defined substrate-binding pocket where the catalytic triad is found within a sheltered, smaller gorge

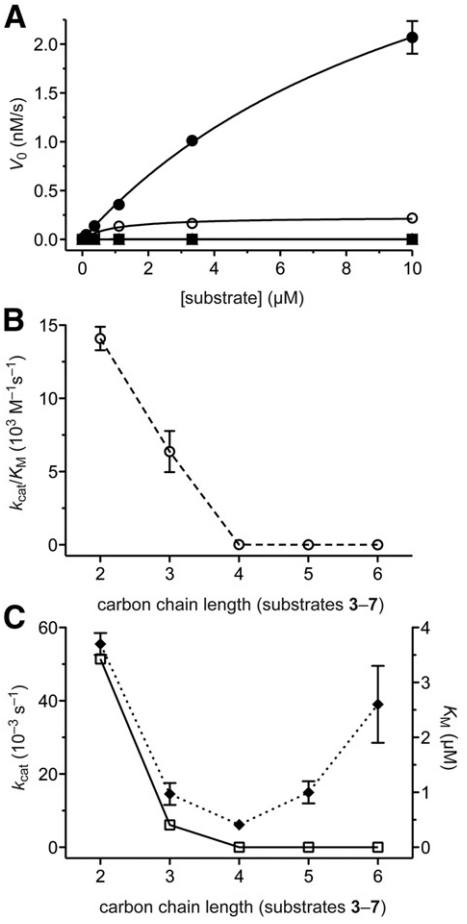

Fig. 2. Kinetic measurements for the substrate specificity of TM0077: A) hydrolysis of fluorogenic esterase substrates by TM0077. Kinetic values are shown ± SE and the values are fitted to the standard Michaelis–Menten equation. The substrates are shown with the following symbols: substrate **3** (○); substrate **4** (●); substrate **8** (□); substrate **9** (■); and substrate **10** (△). Data fitted using Origin 6.1 (OriginLab Corp., Northampton, MA). **B**) Substrate specificity of TM0077 based on carbon chain length. Overall substrate specificity of TM0077 plotted versus carbon chain length (substrates **3**–**7**) where the carbonyl carbon is defined as carbon 1. Constants determined as in Fig. 2A. C) Individual rate constants for the hydrolysis of substrates **3**–**7** versus the carbon chain length. Values for k_{cat} shown with (□) and scale given on the left y-axis. Values for K_m shown with (♦) and scale given on the right y-axis. All values are shown ± SE.

(Fig. 3A–C) [8]. By combining the structural information about the binding pocket residues and their amino acid conservation, eight amino acids residues (Asn88, Tyr92, Trp102, Trp105, Trp124, Phe213, Pro228, and Ile276) were chosen for this study that define the walls of the larger substrate binding pocket, are located near the nucleophilic serine, and show reasonable sequence conservation (Table 2; Fig. 3). These eight amino acids were hypothesized to regulate the unusual substrate specificity of TM0077. Each of these amino acids was then converted separately to alanine and the kinetics of enzymatic catalysis by these variants of TM0077 and combinatorial double alanine variants of TM0077 were measured against substrates **1**–**3** to determine their importance to alcohol recognition and to substrates **8** and **9** to determine their importance to ester recognition (Fig. 4). Substrates **8** and **9** were chosen for further analysis of ester recognition because they contain branched ester moieties and displayed low, but measurable, catalytic activity with the wild-type enzyme (Table 1).

Kinetic measurement with the TM0077 variants shows that the large hydrophobic section of the TM0077 binding pocket contributes little to the catalytic activity of TM0077, as substitution of Asn88, Trp102, Trp105, and Trp124 with alanine changed the catalytic efficiency toward the three acetate substrates **1**–**3** by less than 10-fold (Fig. 4A). This minor affect of multiple nonconservative substitutions on the catalytic activity of TM0077 suggests that the substrate-binding surface has been evolutionarily tuned to provide robust substrate recognition and catalytic activity [24]. Similar large, hydrophobic binding pockets with a minimal number of hydrogen bonding groups are known to facilitate broad substrate specificity [25,26].

The large binding pocket of TM0077 then narrows at one end to a small gorge defined by the side-chain atoms on Tyr92, Phe213, Pro228 and Ile276 (Fig. 3) where irreversible inhibitors and transition state mimics are known to bind [8,12]. Among these amino acids, proper substrate positioning by Pro228 and Ile276, whose side-chains define the sides of the catalytic gorge, are most important to the catalytic activity of TM0077 (Fig. 3C and D). Substitution of either Pro228 or Ile276 significantly reduced (>10-fold) the catalytic efficiency of TM0077 toward all three acetate substrates (Fig. 4A). Thus, the large surface area of the binding pocket determines the broad specificity of TM0077 toward diverse alcohol scaffolds, but only Pro228 and Ile276 appear to play a major role in controlling the narrow specificity of TM0077 toward acetate containing substrates.

As further confirmation of their roles in the deacetylation reaction, these amino acid substitutions (Y92A, F213A, P228A, and I276A) were combined into double alanine-substituted variants and the catalytic activity of the variants measured against substrate **3** (Y92A P228A TM0077, F213A P228A TM0077, or P228A I276A TM0077). Each of the double alanine variants further decreased the catalytic activity of TM0077 toward substrate **3** (Supplemental Table 3) and all combinations of double alanine variants were worse than any single substitution individually. Overall, the substrate specificity of TM0077 was defined by only a few key substrate-binding residues.

3.3. Structural basis for the narrow substrate specificity for esters

To understand the structural features that control the narrow substrate specificity of TM0077 for acetate esters, we searched for amino acid substitutions that could broaden the substrate specificity [24], and focused on potential plasticity residues near the active site [27]. Similar to the reaction with diverse alcohols, Pro228 and Ile276 had the largest affect on the hydrolytic rate and the greatest control of the narrow substrate specificity of TM0077 (Fig. 4B and Supplemental Table 6). Whereas, wild-type TM0077 shows fairly narrow specificity toward acetyl and propyl esters with steep drops in catalytic activity toward sterically bulky or hindered substrates like substrates **8** and **9** (Table 1 and Fig. 1B), the P228A and I276A variants of TM0077 retained much higher relative catalytic activities toward substrates **8** and **9** (Fig. 4B and Supplemental Table 6). For instance, P228A decreased the activity of TM0077 against substrate **3** by 33-fold, but it only lowered the activity against substrate **8** by 8-fold. For substrate **9**, the P228A variant had 4-fold higher enzymatic efficiency ($k_{cat}/K_M = 95\ M^{-1}\ s^{-1}$) than wild-type TM0077 and the double alanine variants (Y92A/P228A, F213A/P228A, and I276A/P228A) had only small differences in k_{cat}/K_M values (0.8-fold to 1.6-fold) from wild-type TM0077 and these differences were smaller than either of the single mutations independently.

Residues Ile276 and especially Pro228 can thus be classified as plasticity residues, as single substitutions shifted the substrate specificity of TM0077 [27]. Although the P228A and I276A variants are trading low substrate turnover (low k_{cat}) for broadened specificity, such trade-offs are common in plasticity residues near the active site that make direct contact with the substrate [28]. Pro228 is an unusual plasticity residue due to its proximity to the active site and its lack of conformational flexibility [24]. Pro228 is in the rigid *cis* conformation and its γ and δ carbons define the surface area, directly opposite the nucleophilic serine (Figs. 3B and C). Thus, the rigid substrate-binding surface of Pro228 may correctly position the substrate for reaction with Ser188. Substitution of Pro228 likely removed steric hindrance in the binding pocket to allow the bulkier substrates to access the active site gorge

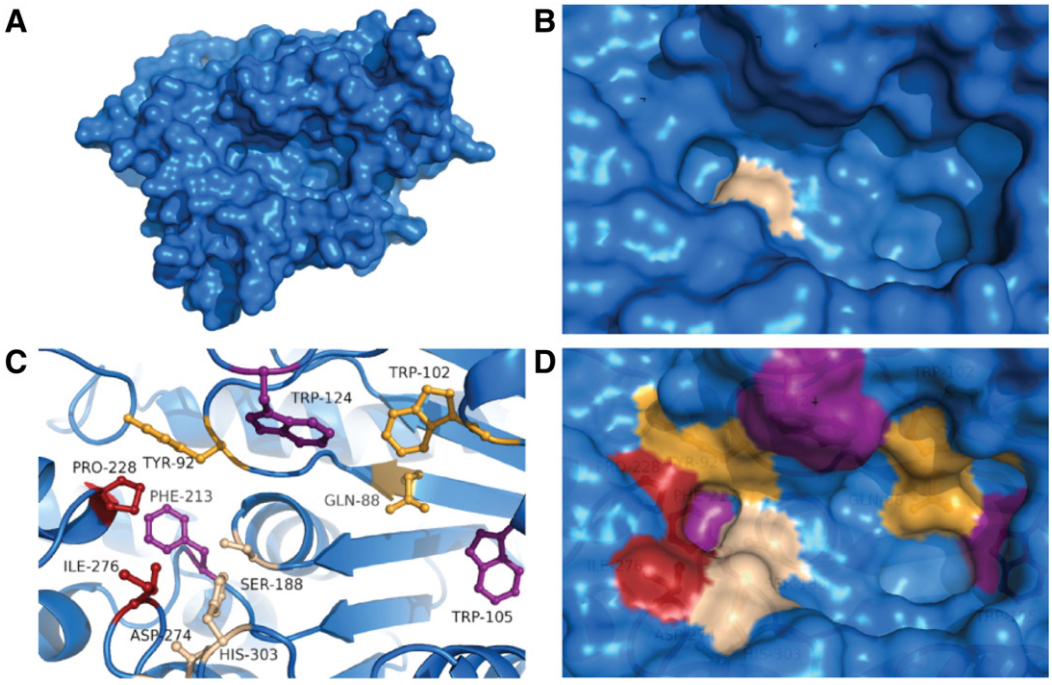

Fig. 3. Substrate recognition by TM0077: A) monomer of TM0077. Surface representations of one monomer of the hexameric structure of TM0077. B) Substrate binding pocket of TM0077. Surface representation of the binding pocket of TM0077 with the catalytic serine nucleophile (Ser188) highlighted in tan. C) Ball and stick representation of the substrate binding pocket of TM0077. TM0077 is oriented identically to part (A). Residues shown in sticks were substituted with alanine and in tan are the catalytic triad residues. Residues colored based on their affect on the enzymatic efficiency of TM0077 hydrolysis of substrate **3**. The residues highlighted in red had k_{cat}/K_m value changes from wild-type greater than ten-fold, in orange had a greater than two-fold change, and in purple had less than a 2-fold change. D) Surface representation of relative kinetic results. Coloration is identical to panel C. Figures made using PDB ID: 1VLQ and PyMol.

and increased the structural plasticity of TM0077 [29]. The γ2 carbon on Ile276 then defines the remaining surface area of the binding pocket and packs against the catalytic histidine (His303). Although, isoleucine is not fully conserved at this position in CE7 acetyl esterases, the branched methyl group that forms the binding surface is completed conserved (Table 2).

4. Conclusion

Together these precise enzyme kinetic measurements combined with the structural and mutagenesis results confirm the unusual substrate specificity of acetyl esterases from CE7 and suggest strict evolutionary selection for the broad substrate specificity for alcohol substituents and for the narrow substrate specificity for ester substituents. Only limited substitutions to the substrate-binding pocket significantly affected this substrate specificity profile and only two plasticity residues, Pro228 and Ile276, control the narrow substrate specificity of TM0077 for acetate esters. Variants of TM0077 with changes at Pro228 and Ile276 present potential starting points for future directed evolution studies, as enzymes with broad specificity increase the likelihood of uncovering novel enzyme functionalities [27,30]. With its broad substrate specificity to diverse alcohol scaffolds and robustness to substitution, this broadened specificity toward sterically hindered ester bonds could make TM0077 a valuable biocatalyst.

Acknowledgments

We thank Andrea Bolen, Ali Donovan, Jessi Grostefon, Erin Hemmelgarn, Stephanie Knezz, Brent Kochert, Alicia Phelps, Bri Richine, and Ariel Tyring for assistance with preliminary enzyme purification and enzymatic analysis. M.A.H. was supported by a Butler Summer Institute Scholarship. A.M.G. was supported by a Holcomb grant from Butler University. R.J.J. was supported by start-up funds and a Holcomb grant from Butler University and a Senior Research Grant from the Indiana Academy of Sciences. C.T.A. and L.D.L. were supported by the Howard Hughes Medical Institute.

Table 2
Amino acid conservation among acetyl esterases from CE7 based on ClustalW alignment to TM0077 from *Thermotoga maritima*.

	Amino acid residue number in TM0077[a]											Identity (%)
	88	92	102	105	124	145	186–192	213	228	229	276	
Thermotoga maritima	Q	Y	W	W	W	M	GGSQGGG	F	P	Y	I	
Thermotoga neapolitana	Q	Y	W	W	W	M	GGSQGGG	F	P	Y	I	90
Streptomyces coelicolor	E	Y	H	W	W	M	GASQGGG	F	P	Y	T	54
Bacillus subtilis	K	Y	M	W	–	M	GGSQGGG	Y	P	Y	V	42
Bacillus pumilus	R	Y	I	W	–	M	GGSQGGA	Y	P	Y	I	41
Thermoanaerobacterium	R	Y	K	Y	–	I	GPSQGGG	F	N	Y	V	33
Enterococcus faecalis	D	Y	F	W	–	M	GGSQGGG	S	G	Y	I	31
Clostridium perfringens	E	Y	N	Y	–	I	GGSQGGA	F	D	Y	I	30
Streptococcus pneumoniae	H	Y	M	F	–	I	GASQGGA	F	E	Y	V	30
Leptospira interrogans	Y	Y	I	L	L	F	GKSMGAS	N	S	M	I	25

[a] The amino acid sequence of TM0077 was aligned using ClustalW to nine other acetyl xylan esterases [19]. The sequence identity of the amino acids in the TM0077 binding pocket is highlighted. The amino acid numbering corresponds to the amino acid numbering in TM0077. The full sequence alignment is given in Supplemental Fig. 3.

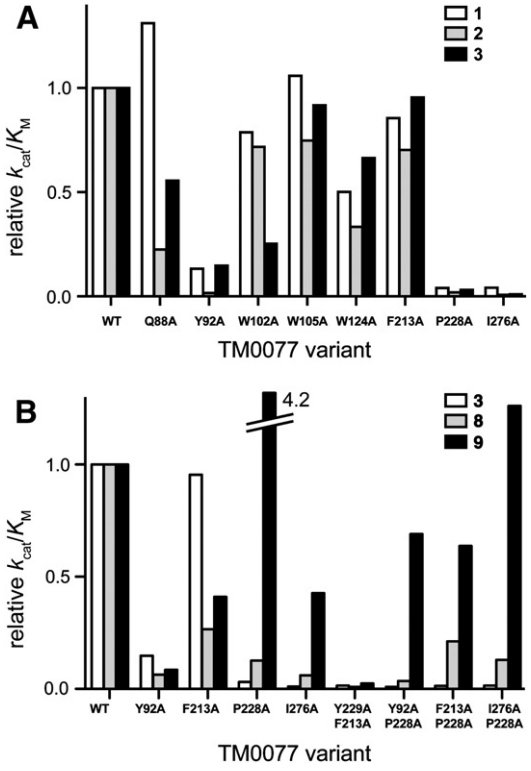

Fig. 4. Substrate specificity of TM0077 variants: A) comparison of the enzymatic efficiency (k_{cat}/K_m) of variants of TM0077 against substrates **1**–**3**. All enzymatic efficiency values for TM0077 variants were normalized based on the enzymatic efficiency of wild-type TM0077 against each substrate (Table 1). Kinetic values for each TM0077 variant and substrate are given in Supplemental Tables 3–5. B) Comparison of the enzymatic efficiency (k_{cat}/K_m) of variants of TM0077 against substrates **3**, **8**, and **9**. All enzymatic efficiency values for TM0077 variants were normalized based on the enzymatic efficiency of wild-type TM0077 against each substrate. Kinetic values for each TM0077 variant and substrate are given in Supplemental Table 6.

Appendix A. Supplementary data

Supplementary data to this article can be found online at http://dx.doi.org/10.1016/j.bbapap.2012.05.009.

References

[1] E. Kuznetsova, M. Proudfoot, S.A. Sanders, J. Reinking, A. Savchenko, C.H. Arrowsmith, A.M. Edwards, A.F. Yakunin, Enzyme genomics: application of general enzymatic screens to discover new enzymes, FEMS Microbiol. Rev. 29 (2005) 263–279.
[2] U.T. Bornscheuer, Microbial carboxyl esterases: classification, properties and application in biocatalysis, FEMS Microbiol. Rev. 26 (2002) 73–81.
[3] E. Busto, V. Gotor-Fernandez, V. Gotor, Hydrolases: catalytically promiscuous enzymes for non-conventional reactions in organic synthesis, Chem. Soc. Rev. 39 (2010) 4504–4523.
[4] H. Jochens, M. Hesseler, K. Stiba, S.K. Padhi, R.J. Kazlauskas, U.T. Bornscheuer, Protein engineering of alpha/beta-hydrolase fold enzymes, ChemBioChem 12 (2011) 1508–1517.
[5] R. Kourist, H. Jochens, S. Bartsch, R. Kuipers, S.K. Padhi, M. Gall, D. Bottcher, H.J. Joosten, U.T. Bornscheuer, The alpha/beta-hydrolase fold 3DM database (ABHDB) as a tool for protein engineering, ChemBioChem 11 (2010) 1635–1643.
[6] F. Vincent, S.J. Charnock, K.H. Verschueren, J.P. Turkenburg, D.J. Scott, W.A. Offen, S. Roberts, G. Pell, H.J. Gilbert, G.J. Davies, J.A. Brannigan, Multifunctional xylooligosaccharide/cephalosporin C deacetylase revealed by the hexameric structure of the *Bacillus subtilis* enzyme at 1.9 Å resolution, J. Mol. Biol. 330 (2003) 593–606.
[7] P. Biely, J. Puls, H. Schneider, Acetyl xylan esterase in fungal cellulolytic systems, FEBS Lett. 186 (1985) 80–84.
[8] M. Levisson, G.W. Han, M.C. Deller, Q. Xu, P. Biely, S. Hendriks, L.F. Ten Eyck, C. Flensburg, P. Roversi, M.D. Miller, D. McMullan, F. von Delft, A. Kreusch, A.M. Deacon, J. van der Oost, S.A. Lesley, M.A. Elsliger, S.W. Kengen, I.A. Wilson, Functional and structural characterization of a thermostable acetyl esterase from *Thermotoga maritima*, Proteins 80 (2012) 1545–1559.
[9] G. Degrassi, M. Kojic, G. Ljubijankic, V. Venturi, The acetyl xylan esterase of *Bacillus pumilus* belongs to a family of esterases with broad substrate specificity, Microbiology 146 (Pt 7) (2000) 1585–1591.
[10] I. Martinez-Martinez, S. Montoro-Garcia, J.D. Lozada-Ramirez, A. Sanchez-Ferrer, F. Garcia-Carmona, A colorimetric assay for the determination of acetyl xylan esterase or cephalosporin C acetyl esterase activities using 7-amino cephalosporanic acid, cephalosporin C, or acetylated xylan as substrate, Anal. Biochem. 369 (2007) 210–217.
[11] K. Drzewiecki, A. Angelov, M. Ballschmite, K.-J. Tiefenbach, R. Sterner, W. Liebl, Hyperthermostable acetyl xylan esterase, Microb. Biotechnol. 3 (2010) 84–92.
[12] S. Montoro-Garcia, F. Gil-Ortiz, F. Garcia-Carmona, L.M. Polo, V. Rubio, A. Sanchez-Ferrer, The crystal structure of the cephalosporin deacetylating enzyme acetyl xylan esterase bound to paraoxon explains the low sensitivity of this serine hydrolase to organophosphate inactivation, Biochem. J. 436 (2011) 321–330.
[13] L. Tian, Y. Yang, L.M. Wysocki, A.C. Arnold, A. Hu, B. Ravichandran, S.M. Sternson, L.L. Looger, L.D. Lavis, Selective esterase-ester pair for targeting small molecules with cellular specificity, Proc. Natl. Acad. Sci. U. S. A. 109 (2012) 4756–4761.
[14] C.N. Pace, F. Vajdos, L. Fee, G. Grimsley, T. Gray, How to measure and predict the molar absorption coefficient of a protein, Protein Sci. 4 (1995) 2411–2423.
[15] H. Edelhoch, Spectroscopic determination of tryptophan and tyrosine in proteins, Biochemistry 6 (1967) 1948–1954.
[16] S.C. Gill, P.H. von Hippel, Calculation of protein extinction coefficients from amino acid sequence data, Anal. Biochem. 182 (1989) 319–326.
[17] D.S. Froese, S. Healy, M. McDonald, G. Kochan, U. Oppermann, F.H. Niesen, R.A. Gravel, Thermolability of mutant MMACHC protein in the vitamin B12-responsive cblC disorder, Mol. Genet. Metab. 100 (2010) 29–36.
[18] F.H. Niesen, H. Berglund, M. Vedadi, The use of differential scanning fluorimetry to detect ligand interactions that promote protein stability, Nat. Protoc. 2 (2007) 2212–2221.
[19] R. Chenna, H. Sugawara, T. Koike, R. Lopez, T.J. Gibson, D.G. Higgins, J.D. Thompson, Multiple sequence alignment with the Clustal series of programs, Nucleic Acids Res. 31 (2003) 3497–3500.
[20] M. Levisson, L. Sun, S. Hendriks, P. Swinkels, T. Akveld, J.B. Bultema, A. Barendregt, R.H.H. van den Heuvel, B.W. Dijkstra, J. van der Oost, Crystal structure and biochemical properties of a novel thermostable esterase containing an immunoglobulin-like domain, J. Mol. Biol. 385 (2009) 949–962.
[21] M. Levisson, J. van der Oost, S.W. Kengen, Carboxylic ester hydrolases from hyperthermophiles, Extremophiles 13 (2009) 567–581.
[22] T. Koseki, Y. Miwa, S. Fushinobu, K. Hashizume, Biochemical characterization of recombinant acetyl xylan esterase from *Aspergillus awamori* expressed in *Pichia pastoris*: mutational analysis of catalytic residues, Biochim. Biophys. Acta 1749 (2005) 7–13.
[23] Y.Z. Yang, P. Babiak, J.L. Reymond, New monofunctionalized fluorescein derivatives for the efficient high-throughput screening of lipases and esterases in aqueous media, Helv. Chim. Acta 89 (2006) 404–415.
[24] O. Khersonsky, C. Roodveldt, D. Tawfik, Enzyme promiscuity: evolutionary and mechanistic aspects, Curr. Opin. Chem. Biol. 10 (2006) 498–508.
[25] S. Copley, Enzymes with extra talents: moonlighting functions and catalytic promiscuity, Curr. Opin. Chem. Biol. 7 (2003) 265–272.
[26] I. Nobeli, A.D. Favia, J.M. Thornton, Protein promiscuity and its implications for biotechnology, Nat. Biotechnol. 27 (2009) 157–167.
[27] Y. Yoshikuni, T.E. Ferrin, J.D. Keasling, Designed divergent evolution of enzyme function, Nature 440 (2006) 1078–1082.
[28] J.E. Vick, D.M. Schmidt, J.A. Gerlt, Evolutionary potential of (beta/alpha)8-barrels: *in vitro* enhancement of a "new" reaction in the enolase superfamily, Biochemistry 44 (2005) 11722–11729.
[29] A. Nath, W.M. Atkins, A quantitative index of substrate promiscuity, Biochemistry 47 (2008) 157–166.
[30] C.A. Tracewell, F.H. Arnold, Directed enzyme evolution: climbing fitness peaks one amino acid at a time, Curr. Opin. Chem. Biol. 13 (2009) 3–9.